

Multivariate genome-wide association study identifies 780 unique genetic loci associated with cortical morphology

Authors: Alexey A. Shadrin, Ph.D.^{1*}, Tobias Kaufmann, Ph.D.¹, Dennis van der Meer, Ph.D.^{1,2}, Clare E. Palmer, Ph.D.^{3,6}, Carolina Makowski, Ph.D.^{4,6}, Robert Loughnan M.S.¹¹, Terry L. Jernigan, Ph.D.^{6,10,11}, Tyler M. Seibert, M.D. Ph.D.^{4,6,8,9}, Donald J Hagler, Ph.D.^{4,6}, Olav B. Smeland, M.D. Ph.D.¹, Yunhan Chu, Ph.D.¹, Aihua Lin, Ph.D.¹, Weiqiu Cheng, Ph.D.¹, Guy Hindley, M.S.¹, Wesley K. Thompson, Ph.D.^{1,5}, Chun C. Fan, M.D. Ph.D.⁶, Dominic Holland, Ph.D.^{3,4,6}, Lars T. Westlye, Ph.D.^{1,7}, Oleksandr Frei, Ph.D.¹, Ole A. Andreassen, M.D. Ph.D.^{1#*} & Anders M. Dale, Ph.D.^{1,3,4,6#*}

¹ NORMENT Centre, Division of Mental Health and Addiction, Oslo University Hospital & Institute of Clinical Medicine, University of Oslo, Oslo, Norway

² School of Mental Health and Neuroscience, Faculty of Health, Medicine and Life Sciences, Maastricht University, The Netherlands

³ Department of Neurosciences, University of California San Diego, La Jolla, CA 92037, USA

⁴ Department of Radiology, University of California San Diego, La Jolla, CA 92037, USA

⁵ Department of Family Medicine and Public Health, University of California San Diego, La Jolla, CA 92037, USA

⁶ Center for Multimodal Imaging and Genetics, University of California San Diego, La Jolla, CA 92037, USA

⁷ Department of Psychology, University of Oslo, Oslo, Norway

⁸ Department of Bioengineering, University of California San Diego, La Jolla, CA 92037, USA

⁹ Department of Radiation Medicine and Applied Sciences, University of California San Diego, La Jolla, CA 92037, USA

¹⁰ Center for Human Development, University of California San Diego, La Jolla, CA 92037, USA

¹¹ Department of Cognitive Science, University of California San Diego, La Jolla, CA 92037, USA

* Corresponding authors:

Alexey A. Shadrin, Ph.D., e-mail: a.a.shadrin@medisin.uio.no

NORMENT Centre

Building 48, Oslo University Hospital, Ullevål, PO Box 4956 Nydalen, 0424 Oslo, Norway

Tel: +47 922 57 686

Ole A. Andreassen, M.D. Ph.D., email: ole.andreassen@medisin.uio.no

NORMENT Centre

Building 49, Oslo University Hospital, Ullevål, PO Box 4956 Nydalen, 0424 Oslo, Norway

Tel: +47 23 02 73 50 (22 11 78 43 dir)

Fax: +47 23 02 73 33

Anders M. Dale, Ph.D., email: andersmdale@gmail.com

Center for Translational Imaging and Precision Medicine, Center for Multimodal Imaging and Genetics, Dept. of Neuroscience and Radiology, University of California San Diego
9452 Medical Center Dr, La Jolla, CA 92037, United States

Tel: (858) 822-6671

Fax: (858) 534-1078

These authors contributed equally to this work.

Word count: abstract 148; main 3407; figures 3; references 27.

Abstract

Brain morphology has been shown to be highly heritable, yet only a small portion of the heritability is explained by the genetic variants discovered so far. Here we exploit the distributed nature of genetic effects across the brain and apply the Multivariate Omnibus Statistical Test (MOSTest) to genome-wide association studies (GWAS) of vertex-wise structural magnetic resonance imaging (MRI) cortical measures from N=35,657 participants in the UK Biobank. We identified 695 loci for cortical surface area and 539 for cortical thickness, in total 780 unique genetic loci associated with cortical morphology. This reflects an approximate 10-fold increase compared to the commonly applied univariate GWAS methods. Power analysis indicates that applying MOSTest to vertex-wise structural MRI data triples the effective sample size compared to conventional univariate GWAS approaches. Functional follow up including gene-based analyses implicate 10% of all protein-coding genes and point towards pathways involved in neurogenesis and cell differentiation.

Introduction

Variability in brain morphology is highly heritable, with twin studies estimating heritability for global measures at 89% for total surface area and 81% for mean cortical thickness¹ and regional measures (adjusting for whole brain measures) at up to 46% for cortical area and 57% for thickness². GWAS is a powerful tool for identifying genetic variants that shape the human cortex, but the full breadth of reported heritability estimates has yet to be uncovered. The most recent large-scale GWAS of brain MRI data (N=51,665) from the ENIGMA consortium identified 187 and 50 loci associated with global and regional cortical surface area and thickness, respectively³. The relatively low yield despite high heritabilities of brain morphology is likely due to high polygenicity and small effect size (discoverability) per locus⁴.

Both imaging genetics⁴ and gene expression studies⁵ suggest that genetic effects are distributed across cortical regions, such that variants influencing one cortical region are also likely to affect other cortical regions. Multivariate statistical methods are naturally tailored to model distributed and pleiotropic genetic effects. We recently developed a Multivariate Omnibus Statistical Test (MOSTest)⁶ that aggregates effects across spatially distributed phenotypes, such as cortical thickness, boosting our ability to detect variant-phenotype associations. We showed that applying MOSTest to cortical morphology region of interest (ROI) measures in the UK Biobank substantially increased loci discovery⁶ compared to the commonly applied approach used by the ENIGMA consortium³, here referred to as the min-P approach. For each genetic variant tested for association with multiple phenotypes, min-P considers only the most significant p-value and corrects it for the effective number of phenotypes analyzed, thus failing to exploit shared genetic architecture across brain regions. In contrast, MOSTest relies on the distributed nature of genetic influences across brain regions and allows detection of genetic variants with weak effects in multiple brain regions. We have shown that the discoverability of GWAS variants underlying regional

cortical area and thickness depends on the specific parcellation of cortical regions used, and that parcellations based on genetic correlations from twin studies perform better than genetically un-informed schemes⁴. Here we show that the combined genetic yield (number of loci discovered) for cortical area and thickness can be boosted when using MOSTest (yielding a 3.8-fold increase relative to min-P), and boosted further when moving from a region-based approach to a more fine-grained vertex-wise approach (additional 1.8-fold increase). Uncovering the detailed genetic architecture of cortical area and thickness will provide insight into the underlying neurobiology of the human brain, and give a better understanding of brain-related human traits, such as cognition⁷, as well as neurological⁸ and psychiatric diseases⁹.

Results

Genetic loci discovery

Using MOSTest⁶, we performed a multivariate GWAS of cortical morphology, such that the significance of each locus was estimated after aggregating its effects across all vertices (1284 data points each for thickness and area). This was conducted separately for cortical surface area and thickness in 35,657 individuals from UK Biobank. Cortical morphology estimates were residualized for modality-specific global brain measures prior to analysis in order to estimate regional cortical effects relative to global brain measures. Measurements from left and right hemispheres were included separately (not averaged). We identified 695 and 539 loci, respectively, equating to 780 unique loci associated with cortical morphology. Prior to performing the MOSTest analysis, individual cortical area and thickness measures were residualized for age, sex, scanner site, proxy of surface reconstruction quality, the first twenty genetic principal components, and a participant-specific global measure (either total area or average thickness). Measurements from left and right hemispheres were not merged. For comparison, we repeated this procedure aggregating over 68 ROIs from the Desikan-Killiany parcellation. This resulted in the discovery of 370 loci for cortical surface area and 181 loci for cortical thickness, such that the vertex-wise MOSTest

analysis provided a 1.9-fold and 3.0-fold increase in yield over the region-based MOSTest analysis, respectively. Applying the min-P approach to Desikan-Killiany ROIs resulted in further reduction in the number of loci discovered (88 for cortical surface area; 44 for cortical thickness). This represents a 4.2-fold and 4.1-fold decrease compared to the MOSTest ROI-based analysis, and a 7.9-fold and 12.3-fold decrease compared to vertex-wise MOSTest analysis, respectively. Manhattan plots are presented in Fig. 1, with corresponding QQ plots in Supplementary Fig. 1. Numbers of loci discovered with different approaches are shown in Supplementary Table 1. Specific loci discovered in each analysis are listed in Supplementary Tables 2 - 7.

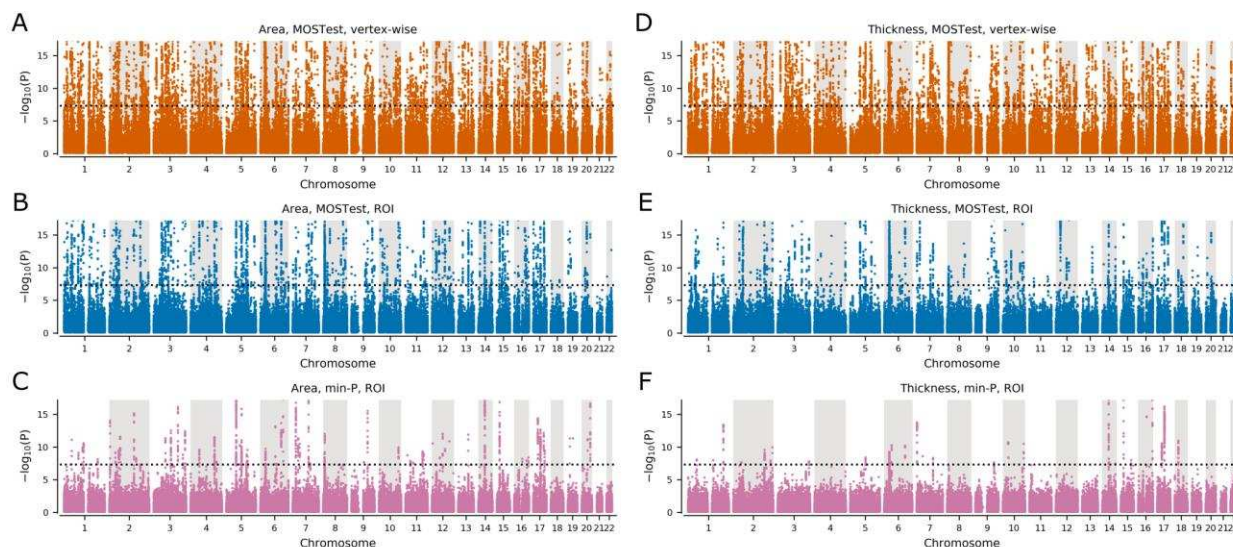


Fig. 1: Manhattan plots for cortical surface area and cortical thickness. (A) Area, MOSTest, vertex-wise: N=695 loci. (B) Area, MOSTest, ROI: N=370 loci. (C) Area, min-P, ROI: N=88 loci. (D) Thickness, MOSTest, VW: N=539 loci. (E) Thickness, MOSTest, ROI: N=181 loci. (F) Thickness, min-P, ROI: N=44 loci. Black dotted horizontal lines show genome-wide significance threshold ($P=5E-8$). Loci; independent genome-wide significant ($P<5E-8$). Y-axes are truncated at $-\log_{10}(P)=17.2$ to highlight the region around genome-wide significance threshold. ROI = region of interest.

To compare the vertex-wise MOSTest results with the most recent ENIGMA GWAS³, we also applied the ENIGMA-based definition of genetic locus. This resulted in 1598 and 1054 unique loci for cortical area and thickness respectively, and a total of 1735 unique loci for cortical morphology identified in the vertex-wise MOSTest analysis (Supplementary Tables 8 - 9).

Power analysis

To estimate the proportion of additive genetic variance explained by genome-wide significant SNPs identified by either MOSTest or min-P as a function of sample size, we used the MiXeR tool¹⁰ (Fig. 2). The horizontal shift of the curve indicates that the effective sample size of MOSTest is around threefold that of min-P. We estimate that with the current UK Biobank sample (N=35,657), 11.6% and 7.0% of the additive genetic variance in cortical surface area and thickness, respectively, can be explained by genome-wide significant loci from the vertex-wise MOSTest analysis. (Fig. 2). In contrast, the min-P approach identifies 1.3% and 0.2% of the explained additive genetic variance for area and thickness, respectively (Fig. 2). The power-analysis indicates that 32.2% and 24.0% of the additive genetic variance in cortical surface area and thickness, respectively, will be discovered in the full UK Biobank sample of N=100,000 using the MOSTest vertex-wise approach (Fig. 2). Further, the proportion of explained variance with the min-P approach in the full UK Biobank sample is estimated to be lower than the yield of MOSTest in the present sample size (Fig. 2).

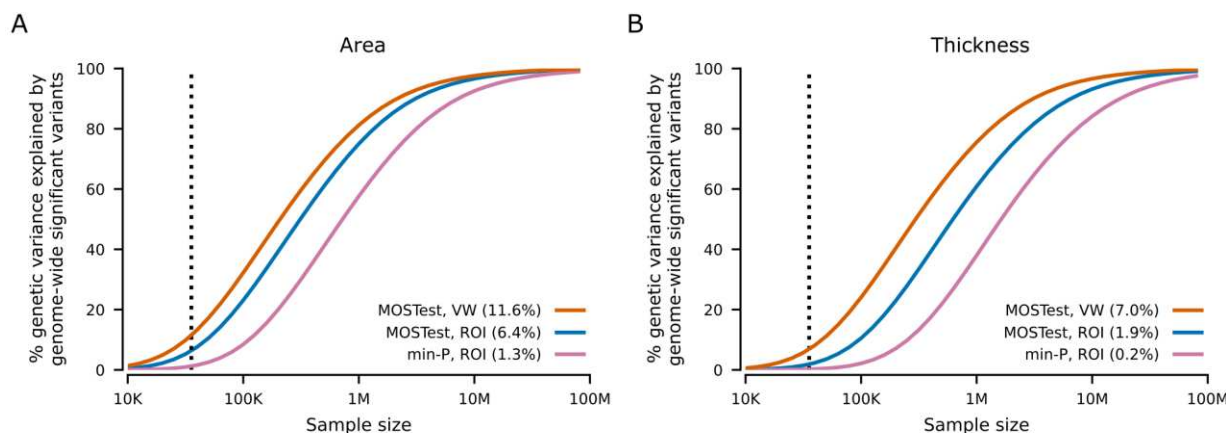


Fig. 2: Estimated percent of additive genetic variance explained by genome-wide significant SNPs as a function of sample size. Percentages of genetic variance explained by identified SNPs ($p < 5E-8$) from multivariate GWAS (MOSTest VW) of area (A) and thickness (B) with current sample size (N=35,657, vertical dotted line) are shown in parentheses, with MOSTest ROI and min-P ROI for comparison. VW = vertex-wise. ROI = region of interest.

Gene-level analysis

Through gene-level analyses of the vertex-wise MOSTest GWAS using MAGMA¹¹, we found that 1647 and 1412 genes, out of a total of 19036 protein-coding genes, were significantly associated with area and thickness, respectively (Supplementary Table 10). We also performed competitive gene-set analyses restricted to the Gene Ontology biological processes category (containing 7343 pathways). This resulted in 204 and 184 significant ($p<0.05/7343$) gene sets associated with area and thickness, respectively. The most significantly associated pathways were related to neuronal development and cell differentiation, with the top 10 shown in Fig. 3.

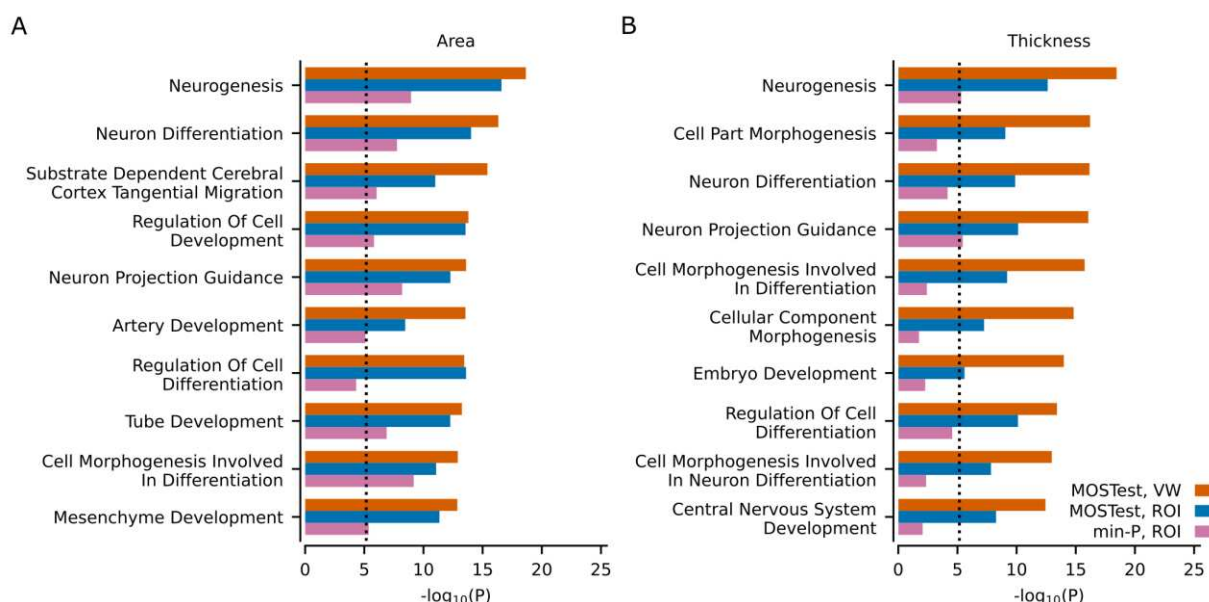


Fig. 3: Gene-set analyses with MAGMA. Results from the gene-set analysis based on multivariate GWA on area (A) and thickness (B). Ten most significant Gene Ontology sets ($N=7343$) in the MOSTest VW analysis are listed on the y-axis, in comparison with MOSTest ROI and min-P ROI. Corresponding uncorrected $-\log_{10}(p\text{-values})$ are shown on the x-axis. P-values were obtained using MAGMA analysis as implemented in FUMA. Vertical dotted line shows Bonferroni correction threshold ($p=0.05/7343$). VW = vertex-wise. ROI = region of interest.

For comparison, we also performed the same analyses on the ROI-based MOSTest and min-P GWAS summary statistics, resulting in 198 area and 66 thickness gene sets for ROI-based MOSTest and 60 area and 4 thickness gene sets for min-P. As shown in Supplementary Figs. 2 and 3, the vertex-wise MOSTest

approach led to much greater significance for nearly all pathways identified. Interestingly, the most significant pathways identified by vertex-wise MOSTest are tightly connected with critical neurobiological processes implicated in brain development while top findings in the min-P analysis are less specific. The distributed effects of identified variants across different brain regions are also illustrated by brain maps, highlighting the mixture of effects across the cortex (Supplementary Fig. 4).

Discussion

We identified 695 loci for cortical surface area and 539 for cortical thickness, in total 780 unique genetic loci associated with cortical morphology. This reflects an approximate 10-fold increase compared to the commonly applied univariate GWAS methods. Our study highlights the greatly improved yield obtained with the multivariate method compared to conventional univariate GWAS approach, which stems from the multivariate nature of brain morphology phenotypes, representing continuous maps per individual. The present results support the hypothesis that the genetic determinants of variability in brain morphology are extensively shared across multiple regions⁶. Our findings further underscore the complex molecular mechanisms shaping the human brain, which we show are largely related to neurodevelopmental processes.

Twin studies have suggested the largely independent nature of cortical surface area and thickness¹. The genetic correlation between them estimated using linkage disequilibrium score regression (LDSR) is $rg=-0.32$ ($p=6.5E-12$)³. Here we identify the specific loci involved and show that these cortical phenotypes share a large proportion of genomic loci. Out of a total of 695 loci for cortical area and 539 loci for cortical thickness, 454 loci (58.2% of the total number of unique loci) were overlapping. These findings illustrate how measures of genetic correlation fail to fully capture the extent to which the genetic influences of two phenotypes are interrelated. LDSR and twin analyses depend on the consistency of effect directions across phenotypes. In contrast, the analysis performed here consider non-null loci as overlapping if they are both

significant and in linkage disequilibrium, regardless of effect directions. Overlapping genetic architecture across brain regions despite the absence of strong genetic correlations are therefore plausible due to common molecular toolkits involved in neurodevelopment across brain regions¹². This is in line with Allen Brain Atlas maps of the adult human brain¹³, showing regions with high similarity in gene expression between cortical structures consistent with the notion that the basic architecture across the entire cortex is similar or “canonical”¹⁴. This may also explain the shared genetic architecture observed for many brain-related traits and disorders¹⁵⁻¹⁷. Accounting for the distributed signal across the cortex in a multivariate framework allowed us to boost power for discovery compared to traditional univariate approaches, such as min-P.

Our gene-level analyses indicated that, with the current sample size, 10% of all protein-coding genes were significantly associated with brain morphology (either cortical area or thickness). Gene-set analyses for both area and thickness confirmed involvement of pathways recently reported by ENIGMA³, but with greater statistical significance. We additionally found strong evidence for the involvement of several genetic pathways regulating neuronal development and differentiation that were not identified by the min-P approach, implicating key biological processes regulating human surface area expansion and increases in thickness. This also corroborates the strong statistical signals and suggests that we are capturing true biological mechanisms that were missed by previous methodologies. These novel findings of neurobiological underpinnings associated with brain morphology provide a framework for follow-up experimental studies to identify the complex polygenic mechanisms involved in human brain development¹⁸. Further, the findings implicating neuronal development and cell differentiation can facilitate experimental studies to gain better insight into the pathobiological mechanisms of brain-related diseases including psychiatric disorders¹⁹, where we need to understand the role of polygenic mechanisms²⁰.

Compared to the current largest brain morphology GWAS (N=50K)³, analyzing parcellation-free, vertex-wise data with MOSTest increased the yield of significant loci 8.5-fold for cortical surface area and 21.1-fold for cortical thickness, despite the lower sample size in our study (N=35K). Of note, while being generally consistent, our protocol differs in a few aspects from the previous GWAS³, where global measures were included in the principal analysis and data for cortical regions were averaged across right and left hemispheres. Using the Desikan-Killiany parcellation approximately 2.0 times more variants were identified for cortical surface area than for cortical thickness both with the min-P and the MOSTest (Supplementary Table 1). In contrast, there were 1.3 times more loci for area compared to thickness when using the MOSTest for parcellation-free vertex-wise data. (Supplementary Table 1). The observed difference in loci yield may be due to differing degrees of mismatch between parcellation schemes and actual architecture of the phenotypes. This seems to be particularly relevant for thickness, where variant effects obtained from an ROI parcellation scheme may be underestimated compared to the vertex-wise approach. This result may explain why parcellation schemes better reflecting the genetic architecture of the cortex improve detectability in imaging genetics studies⁴.

The boost in statistical power using the multivariate vertex-wise approach is equivalent to a more than three-fold increase in effective sample size for both area and thickness (Fig. 2). Our analysis suggests that the substantial gain in power provided by MOSTest is projected to explain approximately 32.2% and 24.0% of the additive genetic variance for cortical surface area and thickness, respectively, upon completion of UK Biobank's target neuroimaging sample (N=100,000)²¹ (Fig. 2). It is possible that multivariate approaches will also boost discovery of genetic associations with other human phenotypes that exhibit shared signal between traits.

To conclude, we have identified 780 unique loci associated with human brain morphology, highlighting its polygenic nature and providing the foundation for functional follow-up experiments. While this study is focused solely on UK Biobank, the generalizability and flexibility of this approach allows its incorporation

into large-scale meta-analyses like ENIGMA²², offering unique opportunities for major advances in our understanding of the genetic determinants of brain morphology.

Materials and Methods

Sample

Genotypes, MRI scans, demographic and clinical data were obtained from the UK Biobank under accession number 27412. For this study, we selected white British individuals (as derived from both self-declared ethnicity and principal component analysis²³) who had undergone the neuroimaging protocol. The resulting sample contained 35,657 individuals with a mean age of 64.4 years (standard deviation 7.5 years), 51.7% female.

Data processing

T1-weighted structural MRI scans were processed with the FreeSurfer v5.3 standard “recon-all” processing pipeline²⁴ to generate 1284 non-smoothed vertex-wise measures (ico3 downsampling with the medial wall removed) and 68 ROI measures (based on the Desikan-Killiany parcellation) summarizing cortical surface area and thickness. All measures were pre-residualized for age, sex, scanner site, a proxy of surface reconstruction quality (FreeSurfer’s Euler number²⁵), the first twenty genetic principal components, and a global measure specific to each set of variables: total cortical surface area and mean cortical thickness for the regional area and thickness measurements correspondingly. Subsequently, a rank-based inverse normal transformation was applied to the residualized measures. We used UK Biobank v3 imputed genotype data²³, carrying out standard quality-checks as described previously⁶, and setting a minor allele frequency threshold of 0.5%, leaving 9 million variants. Variants were tested for association with cortical surface area and cortical thickness at each vertex and each ROI separately using the standard

univariate GWAS procedure. Resulting univariate p-values and effect sizes were further combined in the MOSTest and min-P analyses to identify area- and thickness-associated loci.

MOSTest analysis

Consider N variants and M (pre-residualized) phenotypes. Let z_{ij} be a z-score from the univariate association test between i^{th} variant and j^{th} (residualized) phenotype and $z_i = (z_{i1}, \dots, z_{iM})$ be the vector of z-scores of the i^{th} variant across M phenotypes. Let $Z = \{z_{ij}\}$ be the matrix of z-scores with variants in rows and phenotypes in columns. For each variant consider a random permutation of its genotypes and let $\tilde{Z} = \{\tilde{z}_{ij}\}$ be the matrix of z-scores from the univariate association testing between variants with permuted genotypes and phenotypes. A random permutation of genotypes is done once for each variant and the resulting permuted genotype is tested for association with all phenotypes, therefore preserving correlation structure between phenotypes.

Let \tilde{R} be the correlation matrix of \tilde{Z} , and $\tilde{R} = USV^T$ is its singular valued decomposition (U and V – orthogonal matrixes, S – diagonal matrix with singular values of \tilde{R} on the diagonal). Consider the regularized version of the correlation matrix $\tilde{R}_r = US_rV^T$, where S_r is obtained from S by keeping r largest singular values and replacing the remaining with r_{th} largest. The MOSTest statistics for i^{th} variant (scalar) is then estimated as $x_i = z_i \tilde{R}_r^{-1} z_i^T$, where regularization parameter r is selected separately for cortical area and thickness to maximize the yield of genome-wide significant loci. In this study we observed the largest yield for cortical surface area with $r=10$; the optimal choice for cortical thickness was $r=20$ (Supplementary Fig. 5). The distribution of the test statistics under null ($CDF_{\text{null}}^{\text{most}}$) is approximated from the observed distribution of the test statistics with permuted genotypes, using the empirical distribution in the 99.99 percentile and Gamma distribution in the upper tail, where shape and scale parameters of Gamma distribution are fitted to the observed data. The p-value of the MOSTest test statistic for the i^{th} variant is then obtained as $p_{\text{MOST}} = CDF_{\text{null}}^{\text{most}}(x_i)$.

min-P analysis

Similar to the MOSTest analysis, consider N variants and M preresidualized phenotypes. Let z_{ij} be a z-score from the univariate association test between i^{th} variant and j^{th} (residualized) phenotype and $z_i = (z_{i1}, \dots, z_{iM})$ be the vector of z-scores of the i^{th} variant across M phenotypes. The min-P statistics for the i^{th} variant is then estimated as $y_i = 2\Phi\left(-\max_{j=1 \dots M}(|z_{ij}|)\right)$, where Φ is a cumulative distribution function of the standard normal distribution. The distribution of the min-P test statistics under null ($CDF_{\text{null}}^{\text{min}-P}$) is approximated from the observed distribution of the test statistics with permuted genotypes, using the empirical distribution in the 99.99th percentile and Beta distribution in the upper tail, where shape parameters of Beta distribution (α and β) are fitted to the observed data. The p-value of the min-P test statistic for the i^{th} variant is then obtained as $p_{\text{min}-P} = CDF_{\text{null}}^{\text{min}-P}(y_i)$.

Locus definition

Genetic loci were defined based on association summary statistics produced with MOSTest and min-P following the protocol implemented in FUMA²⁶ with default parameters. The protocol can be summarized as the following:

1. Independent significant genetic variants are identified as variants with p-value<5E-8 and linkage disequilibrium (LD) $r^2<0.6$ with each other.
2. A subset of these independent significant variants with LD $r^2<0.1$ are then selected as lead variants.
3. For each independent significant variant all candidate variants are identified as variants with LD $r^2\geq0.6$ with the independent significant variant.
4. For a given lead variant the borders of the genomic locus are defined as min/max positional coordinates over all corresponding candidate variants.
5. Loci are then merged if they are separated by less than 250kb.

Alternatively, to facilitate comparison with the current largest brain morphology GWAS³, we also counted genetic loci applying locus definition similar to that used by ENIGMA. Briefly, the association summary statistics produced with either MOSTest or min-P were clumped with PLINK²⁷ using p-value threshold of 5E-8 (--clump-p1) and linkage disequilibrium cutoffs of 1 Mb (--clump-kb) and $r^2 < 0.2$ (--clump-r2). Obtained clumps of variants were considered as independent genome-wide significant genetic loci.

MiXeR analysis

MOSTest and min-P p-values were analyzed with the MiXeR tool¹⁰ to estimate the proportion of additive genetic variance explained by genome-wide significant SNPs as a function of sample size. Right censoring (MiXeR option: --z1max 5.45) was applied to mitigate extreme effects which may lead to biased estimates.

Gene-level analysis

We carried out MAGMA-based gene analyses using default settings, which entail the application of a SNP-wide mean model to GWAS summary statistics, with the use of the 1000 Genomes Phase 3 EUR reference panel. Gene-set analyses were done in a similar manner, restricting the sets under investigation to those that are part of the Gene Ontology biological processes subset (N=7343), as listed in the Molecular Signatures Database (MsigdB) v7.0.

Data availability

The data incorporated in this work were gathered from the public UK Biobank resource.

Code availability

MOSTest code is publicly available at <https://github.com/precimed/mostest> (GPLv3 license).

Acknowledgements

We were funded by the Research Council of Norway (276082, 213837, 223273, 204966/F20, 229129, 249795/F20, 225989, 248778, 249795), the South-Eastern Norway Regional Health Authority (2013-123, 2014-097, 2015-073, 2016-064, 2017-004), Stiftelsen Kristian Gerhard Jebsen (SKGJ-Med-008), the EEA Grant 2014-2021 under the project contract No 6/2019, the European Research Council (ERC) under the European Union’s Horizon 2020 research and innovation programme (ERC Starting Grant, Grant Agreement No. 802998) and National Institutes of Health (R01MH100351, R01GM104400, NIDA/NCI: U24DA041123). This work was partly performed on the TSD (Tjeneste for Sensitive Data) facilities, owned by the University of Oslo, operated and developed by the TSD service group at the University of Oslo, IT-Department (USIT). (tsd-drift@usit.uio.no). Computations were also performed on resources provided by UNINETT Sigma2—the National Infrastructure for High Performance Computing and Data Storage in Norway. This work used the Extreme Science and Engineering Discovery Environment (XSEDE) including COMET and OASYS resources at the UCSD through allocation TG-IBN200001.

Competing Interests

Dr. Andreassen has received speaker’s honorarium from Lundbeck, and is a consultant to HealthLytix. Dr. Dale is a Founder of and holds equity in CorTechs Labs, Inc, and serves on its Scientific Advisory Board. He is a member of the Scientific Advisory Board of Human Longevity, Inc. and receives funding through research agreements with General Electric Healthcare and Medtronic, Inc. The terms of these arrangements have been reviewed and approved by UCSD in accordance with its conflict of interest policies. The other authors declare no competing interests.

References

- 1 Panizzon, M. S., Fennema-Notestine, C., Eyler, L. T., Jernigan, T. L., Prom-Wormley, E., Neale, M., Jacobson, K., Lyons, M. J., Grant, M. D., Franz, C. E., Xian, H., Tsuang, M., Fischl, B., Seidman, L., Dale, A. & Kremen, W. S. Distinct genetic influences on cortical surface area and cortical thickness. *Cereb Cortex* **19**, 2728-2735, doi:10.1093/cercor/bhp026 (2009).
- 2 Eyler, L. T., Chen, C. H., Panizzon, M. S., Fennema-Notestine, C., Neale, M. C., Jak, A., Jernigan, T. L., Fischl, B., Franz, C. E., Lyons, M. J., Grant, M., Prom-Wormley, E., Seidman, L. J., Tsuang, M. T., Fiecas, M. J., Dale, A. M. & Kremen, W. S. A comparison of heritability maps of cortical surface area and thickness and the influence of adjustment for whole brain measures: a magnetic resonance imaging twin study. *Twin Res Hum Genet* **15**, 304-314, doi:10.1017/thg.2012.3 (2012).
- 3 Grasby, K. L., Jahanshad, N., Painter, J. N., Colodro-Conde, L., Bralten, J., Hibar, D. P., Lind, P. A., Pizzagalli, F., Ching, C. R. K., McMahon, M. A. B., Shatokhina, N., Zsembik, L. C. P., Thomopoulos, S. I., Zhu, A. H., Strike, L. T., Agartz, I., Alhusaini, S., Almeida, M. A. A., Alnaes, D., Amlen, I. K. et al. The genetic architecture of the human cerebral cortex. *Science* **367**, doi:10.1126/science.aay6690 (2020).
- 4 van der Meer, D., Frei, O., Kaufmann, T., Chen, C. H., Thompson, W. K., O'Connell, K. S., Monereo Sanchez, J., Linden, D. E. J., Westlye, L. T., Dale, A. M. & Andreassen, O. A. Quantifying the Polygenic Architecture of the Human Cerebral Cortex: Extensive Genetic Overlap between Cortical Thickness and Surface Area. *Cereb Cortex* **30**, 5597-5603, doi:10.1093/cercor/bhaa146 (2020).
- 5 Hawrylycz, M., Miller, J. A., Menon, V., Feng, D., Dolbeare, T., Guillozet-Bongaarts, A. L., Jegga, A. G., Aronow, B. J., Lee, C. K., Bernard, A., Glasser, M. F., Dierker, D. L., Menche, J., Szafer, A., Collman, F., Grange, P., Berman, K. A., Mihalas, S., Yao, Z., Stewart, L. et al. Canonical genetic signatures of the adult human brain. *Nat Neurosci* **18**, 1832-1844, doi:10.1038/nn.4171 (2015).
- 6 van der Meer, D., Frei, O., Kaufmann, T., Shadrin, A. A., Devor, A., Smeland, O. B., Thompson, W. K., Fan, C. C., Holland, D., Westlye, L. T., Andreassen, O. A. & Dale, A. M. Understanding the genetic determinants of the brain with MOSTest. *Nat Commun* **11**, 3512, doi:10.1038/s41467-020-17368-1 (2020).
- 7 Vuoksimaa, E., Panizzon, M. S., Chen, C. H., Fiecas, M., Eyler, L. T., Fennema-Notestine, C., Hagler, D. J., Jr., Franz, C. E., Jak, A. J., Lyons, M. J., Neale, M. C., Rinker, D. A., Thompson, W. K., Tsuang, M. T., Dale, A. M. & Kremen, W. S. Is bigger always better? The importance of cortical configuration with respect to cognitive ability. *Neuroimage* **129**, 356-366, doi:10.1016/j.neuroimage.2016.01.049 (2016).
- 8 Querbes, O., Aubry, F., Pariente, J., Lotterie, J. A., Demonet, J. F., Duret, V., Puel, M., Berry, I., Fort, J. C., Celsis, P. & Alzheimer's Disease Neuroimaging, I. Early diagnosis of Alzheimer's disease using cortical thickness: impact of cognitive reserve. *Brain* **132**, 2036-2047, doi:10.1093/brain/awp105 (2009).
- 9 Rimol, L. M., Hartberg, C. B., Nesvag, R., Fennema-Notestine, C., Hagler, D. J., Jr., Pung, C. J., Jennings, R. G., Haukvik, U. K., Lange, E., Nakstad, P. H., Melle, I., Andreassen, O. A., Dale, A. M. & Agartz, I. Cortical thickness and subcortical volumes in schizophrenia and bipolar disorder. *Biol Psychiatry* **68**, 41-50, doi:10.1016/j.biopsych.2010.03.036 (2010).
- 10 Frei, O., Holland, D., Smeland, O. B., Shadrin, A. A., Fan, C. C., Maeland, S., O'Connell, K. S., Wang, Y., Djurovic, S., Thompson, W. K., Andreassen, O. A. & Dale, A. M. Bivariate causal mixture model quantifies polygenic overlap between complex traits beyond genetic correlation. *Nat Commun* **10**, 2417, doi:10.1038/s41467-019-10310-0 (2019).
- 11 de Leeuw, C. A., Mooij, J. M., Heskes, T. & Posthuma, D. MAGMA: generalized gene-set analysis of GWAS data. *PLoS Comput Biol* **11**, e1004219, doi:10.1371/journal.pcbi.1004219 (2015).

- 12 Stiles, J. & Jernigan, T. L. The basics of brain development. *Neuropsychol Rev* **20**, 327-348, doi:10.1007/s11065-010-9148-4 (2010).
- 13 Hawrylycz, M. J., Lein, E. S., Guillozet-Bongaarts, A. L., Shen, E. H., Ng, L., Miller, J. A., van de Lagemaat, L. N., Smith, K. A., Ebbert, A., Riley, Z. L., Abajian, C., Beckmann, C. F., Bernard, A., Bertagnolli, D., Boe, A. F., Cartagena, P. M., Chakravarty, M. M., Chapin, M., Chong, J., Dalley, R. A. *et al.* An anatomically comprehensive atlas of the adult human brain transcriptome. *Nature* **489**, 391-399, doi:10.1038/nature11405 (2012).
- 14 The Allen Institute. *The Genetic Geography of the Brain*, <<http://casestudies.brain-map.org/ggb>> (n.d.).
- 15 Watanabe, K., Stringer, S., Frei, O., Umicevic Mirkov, M., de Leeuw, C., Polderman, T. J. C., van der Sluis, S., Andreassen, O. A., Neale, B. M. & Posthuma, D. A global overview of pleiotropy and genetic architecture in complex traits. *Nat Genet* **51**, 1339-1348, doi:10.1038/s41588-019-0481-0 (2019).
- 16 Smeland, O. B., Frei, O., Fan, C. C., Shadrin, A., Dale, A. M. & Andreassen, O. A. The emerging pattern of shared polygenic architecture of psychiatric disorders, conceptual and methodological challenges. *Psychiatr Genet* **29**, 152-159, doi:10.1097/YPG.0000000000000234 (2019).
- 17 Cross-Disorder Group of the Psychiatric Genomics Consortium. Electronic address, p. m. h. e. & Cross-Disorder Group of the Psychiatric Genomics, C. Genomic Relationships, Novel Loci, and Pleiotropic Mechanisms across Eight Psychiatric Disorders. *Cell* **179**, 1469-1482 e1411, doi:10.1016/j.cell.2019.11.020 (2019).
- 18 Silbereis, J. C., Pochareddy, S., Zhu, Y., Li, M. & Sestan, N. The Cellular and Molecular Landscapes of the Developing Human Central Nervous System. *Neuron* **89**, 248-268, doi:10.1016/j.neuron.2015.12.008 (2016).
- 19 Sullivan, P. F. & Geschwind, D. H. Defining the Genetic, Genomic, Cellular, and Diagnostic Architectures of Psychiatric Disorders. *Cell* **177**, 162-183, doi:10.1016/j.cell.2019.01.015 (2019).
- 20 Gandal, M. J. & Geschwind, D. H. Polygenicity in Psychiatry-Like It or Not, We Have to Understand It. *Biol Psychiatry* **89**, 2-4, doi:10.1016/j.biopsych.2020.10.002 (2021).
- 21 Miller, K. L., Alfaro-Almagro, F., Bangerter, N. K., Thomas, D. L., Yacoub, E., Xu, J., Bartsch, A. J., Jbabdi, S., Sotiroopoulos, S. N., Andersson, J. L., Griffanti, L., Douaud, G., Okell, T. W., Weale, P., Dragonu, I., Garratt, S., Hudson, S., Collins, R., Jenkinson, M., Matthews, P. M. *et al.* Multimodal population brain imaging in the UK Biobank prospective epidemiological study. *Nat Neurosci* **19**, 1523-1536, doi:10.1038/nn.4393 (2016).
- 22 Thompson, P. M., Jahanshad, N., Ching, C. R. K., Salminen, L. E., Thomopoulos, S. I., Bright, J., Baune, B. T., Bertolin, S., Bralten, J., Bruin, W. B., Bulow, R., Chen, J., Chye, Y., Dannlowski, U., de Kovel, C. G. F., Donohoe, G., Eyler, L. T., Faraone, S. V., Favre, P., Filippi, C. A. *et al.* ENIGMA and global neuroscience: A decade of large-scale studies of the brain in health and disease across more than 40 countries. *Transl Psychiatry* **10**, 100, doi:10.1038/s41398-020-0705-1 (2020).
- 23 Bycroft, C., Freeman, C., Petkova, D., Band, G., Elliott, L. T., Sharp, K., Motyer, A., Vukcevic, D., Delaneau, O., O'Connell, J., Cortes, A., Welsh, S., Young, A., Effingham, M., McVean, G., Leslie, S., Allen, N., Donnelly, P. & Marchini, J. The UK Biobank resource with deep phenotyping and genomic data. *Nature* **562**, 203-209, doi:10.1038/s41586-018-0579-z (2018).
- 24 Desikan, R. S., Segonne, F., Fischl, B., Quinn, B. T., Dickerson, B. C., Blacker, D., Buckner, R. L., Dale, A. M., Maguire, R. P., Hyman, B. T., Albert, M. S. & Killiany, R. J. An automated labeling system for subdividing the human cerebral cortex on MRI scans into gyral based regions of interest. *Neuroimage* **31**, 968-980, doi:10.1016/j.neuroimage.2006.01.021 (2006).
- 25 Rosen, A. F. G., Roalf, D. R., Ruparel, K., Blake, J., Seelaus, K., Villa, L. P., Cricic, R., Cook, P. A., Davatzikos, C., Elliott, M. A., Garcia de La Garza, A., Gennatas, E. D., Quarmley, M., Schmitt, J. E., Shinohara, R. T., Tisdall, M. D., Craddock, R. C., Gur, R. E., Gur, R. C. & Satterthwaite, T. D.

- Quantitative assessment of structural image quality. *Neuroimage* **169**, 407-418, doi:10.1016/j.neuroimage.2017.12.059 (2018).
- 26 Watanabe, K., Taskesen, E., van Bochoven, A. & Posthuma, D. Functional mapping and annotation of genetic associations with FUMA. *Nat Commun* **8**, 1826, doi:10.1038/s41467-017-01261-5 (2017).
- 27 Chang, C. C., Chow, C. C., Tellier, L. C., Vattikuti, S., Purcell, S. M. & Lee, J. J. Second-generation PLINK: rising to the challenge of larger and richer datasets. *Gigascience* **4**, 7, doi:10.1186/s13742-015-0047-8 (2015).